THE JOURNAL OF PHYSICAL CHEMISTRY B

Article

pubs.acs.org/JPCB

Effect of Linear Elongation on Carbon Nanotube and Polyelectrolyte Structures in PDMS-Supported Nanocomposite LbL Films

Johannes Frueh,*[,†] Naotoshi Nakashima,[‡] Qiang He,[†] and Helmuth Möhwald[§]

[†]Key Laboratory of Microsystems and Microstructures Manufacturing, Ministry of Education, Micro/Nano Technology Research Centre, Harbin Institute of Technology, Yikuang Street 2, Harbin 150080, China

[‡]Department of Applied Chemistry, Graduate School of Engineering, Kyushu University, Fukuoka 819-0395, Japan

[§]Max Planck Institute of Colloids and Interfaces, Am Mühlenberg 1, 14424 Golm/Potsdam, Germany

Supporting Information

ABSTRACT: Polyelectrolyte (PE) multilayer (PEM) thin films prepared by layer-by-layer self-assembly on flexible substrates are exposed to elongation in many fields of technology. Upon elongation, these types of films are showing interesting, but not understood, phenomena, such as controlled wetting, stimuli-responsive nanovalves, and lithography-free surface structuring. To investigate the mechanisms causing these interesting phenomena, we employed spectroscopic investigations of supported PEM films that were prepared from polystyrene sulfonate (PSS)-wrapped single-walled carbon nanotubes (SWNTs) or pyrene-labeled PSS (PSS-PY) and polydiallyldiammonium chloride. Our results show that the SWNTs agglomerated upon deposition into the PEM and showed a strong change in orientation upon uniaxial elongation of the PEM. Upon release of elongation, the resulting wrinkling pattern was changing its wavelength upon time, in the case of the SWNT-containing PEM. Fluorescence measurements of the PSS-PY in the PEM showed that the PEs changed their orientation due to constant mechanical force from elongation up to a time scale of 2 days after beginning the elongation. The results prove that elongated and released PEM films, until now considered static structures, possess strong kinetics, which has to be taken into account for their application.

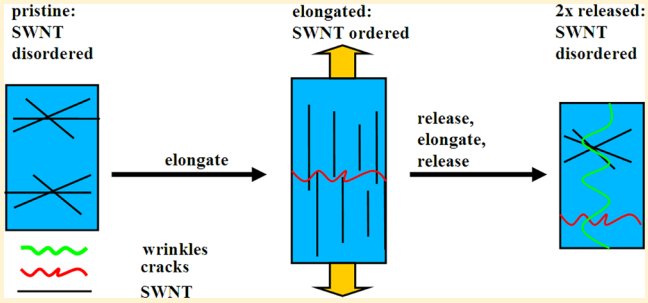

INTRODUCTION

Polyelectrolyte multilayer (PEM) are thin films prepared by sequential adsorption of polyelectrolyte (PE) onto oppositely charged surfaces via the so-called layer-by-layer deposition technique (LbL).[1−3] The process is applied in a cyclic manner, profiting from a surface charge overcompensation, which occurs while PEs are adsorbed at the solid−liquid interface.[1] This allows the structure of PEM to be easily controlled at the molecular level.[2]

The LbL technique has been used successfully for preparation of thin films with film thicknesses up to 1 μm and used for different applications ranging from chemo- or biosensors to coatings of medical implants, which enable cell adhesion and proliferation.[4,5] The versatility of the PEM formation process with respect to the variety of support materials and the possibility of incorporation of different functional species into the PEM results in a high interest of such ultrathin films.[1−3] PEMs with functional entities embedded into the PE matrix possess a number of specific properties, pertaining to their structure, thermodynamics, and electronic, spectroscopic, optical, electromagnetic, and chemical features.[2,6] This provides potential applications of PEM in chemistry, (bio)sensing, and material science.[2,5,6]

For many applications, the films are elongated, and it is of high relevance to control the molecular arrangement during these processes.[7] Studies on mechanical properties of free-standing PEM films prepared as hollow microcapsules were previously performed.[8] The methods concerned application of (isotropic) osmotic pressure and (anisotropic) mechanical pressure, following the change of shape of hollow PEM capsules.[2] More recently, PEMs produced as planar films were exposed to lateral elongation and showed interesting properties, such as formation of stable wrinkles with a regular wave pattern upon elongation and release as well as other effects like controlled wettability.[7,9,10] The Young's modulus was derived from the wrinkling pattern and depends on the type of PE, type of the counterion, ionic strength, and especially the humidity and ranges between 6 MPa and 10 GPa.[2,7,9,11,12] In the case of PEM, chemically linked with embedded SWNTs, even the hardness of ultrahard ceramics was measured.[13] This type of composite is especially interesting, as the two components vastly differ in stiffness and the coupling between the SWNT and PE is most difficult to achieve, but the optical, electrical, and mechanical properties are most promising. Interestingly, in contrast to the mechanical properties, the change of PE organization upon elongation of PEM is still barely investigated.[14,15] The same is valid for particles like SWNTs incorporated into the PEM.[13]

Received: July 19, 2012
Revised: September 5, 2012
Published: September 14, 2012

The aim of the present study is to correlate the lateral elongation of the PEM at a macroscopic level with the ordering and the change of orientation of SWNTs and PE at a molecular level. The SWNTs dispersed in water by PSS wrapping were chosen, since they show, in contrast to chemically linked or oxidized carbon nanotubes, well-separated vibrations.[16,17] Our kinetic studies correlated at macroscopic (change in wrinkling wavelength of up to 2 h) and molecular features (change in excimer peak pronounciation up to 2 days). The samples were exposed to a unidirectional mechanical stress by elongation of up to 10%.

MATERIALS AND METHODS

Pyrene-labeled polystyrene sulfonate (PSS-PY) with a labeling degree of 3% was synthesized by Lidong Li[18] and kindly supplied for the present study. Poly(sodium 4-styrenesulphonate) (PSS) with a molecular weight (MW) of 70 000 g/mol, poly(allyldimethylammonium chloride) (PDDA) (MW = 100 000–200 000 g/mol) as a 20 wt % solution in water, and polyethylenimine (PEI) (MW = 750 000) as a 50 wt % solution in water were purchased from Sigma-Aldrich (Germany). The structures of the used PSS, PSS-PY, and PDDA are summarized in the Supporting Information (Figure S1). Polydimethylsiloxane (PDMS) (Sylgard 184) was purchased from Dow Corning (Midland, MI). Sodium chloride was obtained from Merck KGaA (Darmstadt, Germany). Single-walled carbon nanotubes (HiPico-SWNTs) were purchased from Carbon Nanotechnologies, Inc. (Houston, TX). All chemicals were used without further purification.

The SWNTs were wrapped with PSS in aqueous solution by sonication, followed by centrifugation of nonwrapped SWNTs. Detailed information on the treatment of the PSS wrapping can be found elsewhere.[13] To compare the spectroscopic properties of chemically oxidized and nonoxidized SWNTs, SWNTs were oxidized with ozone. The ozone treatment was done by applying 10 min of ozone to the spread-out SWNT powder. Afterward, the SWNT powder was manually stirred and ozone was again applied for 10 min. This treatment was repeated six times. After this, the SWNTs were dispersed in water by sonication for 1 h, followed by centrifugation for 1 h at 60 000*g* to remove the agglomerated SWNTs. A laboratory water purification system was used to obtain ultrapure water. The specific resistance of the water was above 18.2 MΩ·cm, the pH was 5.5, and the total organic carbon (TOC) value was less than 10 ppb.

PDMS slides were used as the supporting substrate for experiments. The slides were prepared by mixing Dow Corning Sylgard 184 base and curing agent in a 10:1 ratio. The mixture was cast into a form and then cured for 12 h at 60 °C. The obtained PDMS sheets had a thickness of approximately 1 mm.

To test if the wrinkling pattern of the released PEM films changes over time, we employed a similar light-scattering setup like that reported by Nolte et al.[9] The measurement setup can be viewed in the Supporting Information (Figure S2). In our setup, the sample to millimeter-scale paper distance was 11.3 cm, and the used wavelength of the laser was 532 nm. The relation between the wrinkling wavelength and elastic modulus of the film is given by eq 1[7]

$$\bar{E}_f = 3\frac{E_{PDMS}}{1-\nu_f^2}\left(\frac{\lambda}{2\pi d}\right)^3 \quad (1)$$

where E and ν represent the Young's modulus and Poisson's ratio of the film ($_f$) and the PDMS ($_{PDMS}$), respectively. For the dry state, the Poisson's ratio of the PEM is 0.33 and, for the PDMS, 0.5.[7] λ is the wrinkling wavelength, and d is the height of the film (in our case, the height of the film is 233 ± 15 nm) (values from vis light reflectometry; for setup details, see the Supporting Information (page S4) and for theory, see ref 19). The elastic modulus of the PDMS is ∼2.7 ± 0.2 MPa.[7] To measure the kinetics of the wrinkles from the PEM prepared with and without SWNTs, the light-scattering patterns in the released state were analyzed based on their position and width. Since the samples showed very similar scattering patterns, the width of the scattering peak was considered as the error of the experiment.

Sample Preparation. The PEM films were prepared using the LbL deposition procedure.[3] This procedure is based on alternating deposition of anionic and cationic polyelectrolytes. The film formation is driven by electrostatic charge overcompensation.[20] The samples for fluorescence measurements were prepared by dipping, using a DR-3 dipping robot (Riegler & Kirstein, Berlin, Germany), similar to a protocol described elsewhere.[3] The SWNT-containing samples were prepared by spraying deposition with a spraying time of 6 s for all solutions.[21]

The PEI deposition was performed from a salt-free solution of PEI (0.5 g/L) at pH 5. Studies proving the homogeneous film formation on non-plasma-etched surfaces were published recently.[14,22] Despite evidence of a homogeneous PEM film buildup, we would like to mention that we used to integrate over a relatively large film area (ca. 1 cm^2) for fluorescence spectroscopy and also, for UV–vis-NIR spectroscopy, several square millimeters. Therefore, small inhomogeneities in the film structure would not be detected.

The solutions of PSS-SWNT, PSS, PSS-PY, and PDDA contained 0.5 M NaCl. In all solutions (except PSS-PY, which had a PE concentration of 1.3 mg/L (pyrene concentration = 5.09×10^{-5}g/L)), the PE concentration was 0.5 g/L. The samples prepared for fluorescence measurements had a structure of $PDMS/PEI/(PSS\text{-}PY/PDDA)_{16}$. The structure of the SWNT-containing samples was $PDMS/PEI/(PSS\text{-}SWNT/PDDA)_{60}$. Since the PEM is very sensitive to deformation,[15] we would like to mention that the samples were prepared on glass supports to prevent a bending of the PDMS during spraying.

Film Stretching. The deformation of the PEM was performed by uniaxial elongation of the PDMS slides using a homemade stretching device. The measurements were always carried out in the order, 0, 1, 2, 3, 5, 8, and 10% elongation, followed by full release of the force. Since SWNT-containing films are very brittle,[17] and, in many cases, the films are employed in an aqueous environment,[4,5] we elongated these films under water to be able to measure the structural change beyond 1% elongation. At this point, we would like to mention that the sample release was performed in air to observe the wrinkle formation.

The samples were measured in air, and the relative humidity of the surrounding gas atmosphere was in all cases 27.5 ± 2.5%. For fluorescence and UV–vis-NIR absorption measurements, a Rotronic Hygropalm 1 with a Hygroclip SP05 (Rotronic, Bassersdorf, Switzerland) and a THI-HP hygrometer (AS-ONE, Osaka, Japan) were used, respectively. The fluorescence measurements were made with a Horiba Jobin Yvon Fluoromax 3 (Horiba, Kyoto, Japan) fluorescence spectrometer. The UV–vis-NIR measurements were made with a home-built diode array spectrometer. The software to subtract the PDMS and PEM background from the SWNTs was OPUS, version 5.12, from Bruker, (Billerica, MA).

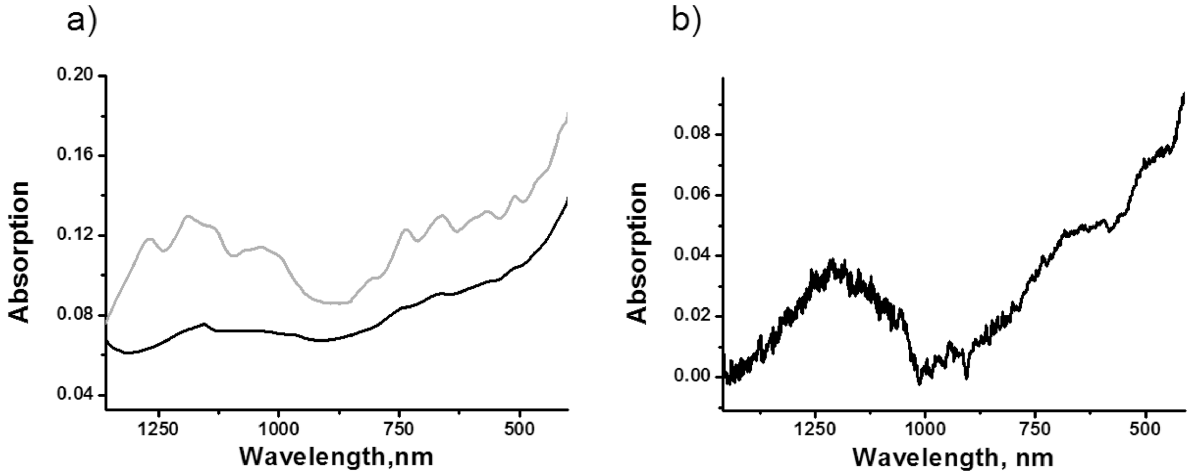

Figure 1. UV−vis-NIR spectra of (a) SWNTs in solution (gray line: PSS-wrapped SWNTs (PSS-SWNTs); black line: chemically oxidized SWNTs) and (b) 60 bilayer-PSS-SWNTs-PDDA film. Assembly of PSS-wrapped SWNTs causes agglomeration of the SWNTs and a higher peak broadening than chemical oxidation of SWNTs.

RESULTS AND DISCUSSION

Alignment of SWNTs in the PEM. To study the alignment of SWNTs in the PEM, the absorption spectra of SWNTs containing PEM were compared to a PSS-SWNT suspension as well as to a solution of ozone-oxidized SWNTs. As shown in Figure 1, the dissolved PSS-wrapped SWNTs exhibit separated peaks, in contrast to ozone-oxidized SWNTs. The absorption peaks of SWNTs within the film are smeared out. This loss of spectral resolution can be explained by aggregation of the unpolar SWNTs in the highly polar PEM film. This aggregation in the film leads to strongly hindered vibrations of the SWNTs and, therefore, to a higher spectral broadening. Interestingly, this agglomeration-based hindrance of vibrations was more severe than the vibration hindrance caused by ozone oxidation (see Figure 1) or the physical entrapment into a polymerized plastic film, as published elsewhere in ref 23.

Orientation Change of SWNTs in a PEM−SWNT Composite Film upon Elongation. To study the change in SWNT orientation upon elongation, the dichroic ratio (ratio between the absorption intensity of vertical (v) and parallel polarized light (p)) was determined based on the SWNT absorption peak at 1114 nm.[24] In this area, no absorption of the PDMS or the PEM was determined in the pristine as well as the elongated state, as can be seen in the Supporting Information (Figure S3a−c). Interestingly, we found very high deviations in the dichroic ratio of our pristine samples, as it is shown in the Supporting Information (Figures S3b,c and S4a,b). This was probably due to the nonconstant amount of downward flowing solution (difference in solution amount depended on the position to the spraying cone and was up to 50%) caused by the manual sample preparation, as well as the positioning of our samples where we tried to cover the whole spraying range to ensure reproducibility of the test. The different speeds of the downward flowing solution influence the nanotube orientation upon deposition onto the sample, whereby the slower the downward flow is, the more arbitrary the nanotube orientation is.

Because of this reason, the obtained error bars were large, and the total change of the SWNT orientation upon elongation was within the error bars; see the Supporting Information (Figure S4a). Within our single samples, the error was much smaller, and therefore, the relative change in the SWNT orientation upon elongation was determined. The error bars are the deviations within relative orientation changes upon elongation toward the corresponding pristine sample, determined for two different samples. The trend for arbitrary orientation was, however, visible for all three observed samples.

Upon an elongation of up to 2%, an increase in the Δ dichroic ratio was detected, as shown in Figure 2. This result confirms our theory that the SWNT-containing PEM in the aqueous environment can be elongated beyond 1%. Despite this, the SWNT-containing PEM is still too brittle to be elongated up to 5%, as it is possible in the case of pyrene-labeled PEM, which changes its orientation up to 5% elongation at 25% relative humidity.[15,17] Therefore, ripping of this film is observed before 5% elongation.

At this point, it is important to note that the Δ dichroic ratio refers, in our case, to an increase in the parallel-to-vertical polarized ratio. The total dichroic ratio increased from 0.29 to 0.58, showing that the strongly prealigned SWNTs become more isotropic, as shown in the Supporting Information (Figure S4a).

The angular orientation of the SWNTs was determined by Fraser's approach.[25] Our pristine samples were, due to the spraying deposition method, prealigned in the direction of the solvent flow. Depending on the sample position, the degree of prealignment was between 66.1° and 72.8° and, in all cases, above the isotropic angle of 54°. Interestingly, in all of our samples, the rotational change upon elongation was in the same order, independent from the pristine SWNT orientation. Upon elongations up to 2%, the orientation change of the SWNTs is ca. 3° per 1% elongation; see the Supporting Information (Figure S4b). We interpret the counterintuitive observation that different samples with different pristine SWNT orientations show the same degree of orientation change upon elongation with the fact that our preorientation is low. A preorientation of 18.8° with a 6° rotation change (within the first 2% elongation) is too small to influence our measurement. Liquid crystals for comparison change their orientation by 90°.[26]

The detected rotational change of the SWNTs is ca. 2× stronger and exactly the opposite way as the rotational change of the pyrene marker molecules or the rotation of sulfate groups of PSS within linearly elongated PEMs.[15,22] The reason for the different direction of orientation is the fact small marker molecules feel only the local acting force, which is, in the case of linear elongation, into the direction of elongation. On a larger scale, one has to account that a linear elongation on a flexible

dx.doi.org/10.1021/jp3071458 | J. Phys. Chem. B 2012, 116, 12257−12262

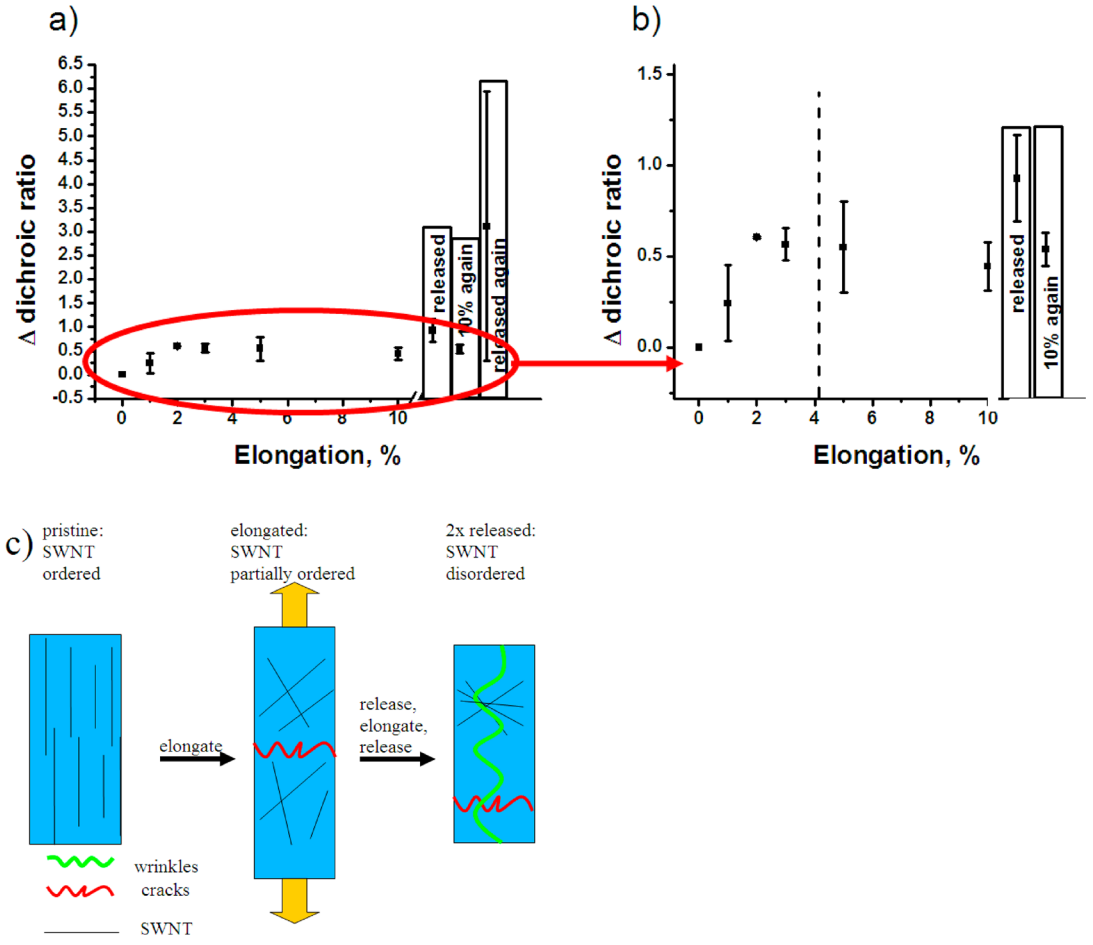

Figure 2. (a) Change in dichroic ratio of the SWNTs (determined from the absorption peak at 1114 nm) embedded within the PEM upon elongation and (b) zoomed-in section of the marked area of (a). The dashed line shows the point of observed breakage of the PEM. In the case of 2% elongation, error bars are within the data point size. (c) Proposed effect of elongation-induced nanotube disordering and, at a later stage, cracks within the PEM; upon a second release, wrinkling and higher nanotube disorder.

substrate is a three-dimensional process, involving compression forces from the sides.

Since the composite PEM is harder than the PDMS support, one expects, therefore, that the evolution of wrinkles upon elongation could explain the observation.[27,28] To our surprise, we did not find such structures, neither in our scattering nor in our microscopic images, as can be seen in the Supporting Information (Figure S5a–d). Since the difference in refractive index between the PEM and water is very low and the PEM is soft in aqueous environments,[15,29] a temporal evolving and rapidly decaying wrinkling structure cannot be excluded; however, it is considered unlikely.

We explain our finding of a gain in isotropic orientation of the SWNTs upon elongation with the fact that the SWNTs are very long rods and span over different areas of the support material. The PDMS we used showed in X-ray reflectometry, close to the surface, a layer of oriented molecules with a higher density than the bulk, that decreases upon elongation.[15] We expect this layer to disintegrate heterogeneously upon elongation, causing sheer forces between the areas, as well as a speed gradient between the disintegrated parts from the border to the center of the sample. As a result, the SWNTs spanning over the disintegrated areas loose their prealignment due to sheer forces, as the Supporting Information (Figure S6) illustrates.

The rotational order of the SWNTs in the PEM decreased upon releasing the PEM film from elongation, as shown in the Supporting Information (Figure S4a,b). This finding is expected, since the wrinkling direction, which was determined by light-scattering (see Figure 3) and microscopic images (data not shown), is perpendicular to the direction of the SWNT ordering. Since scattering effects due to wrinkling formation are unlikely to

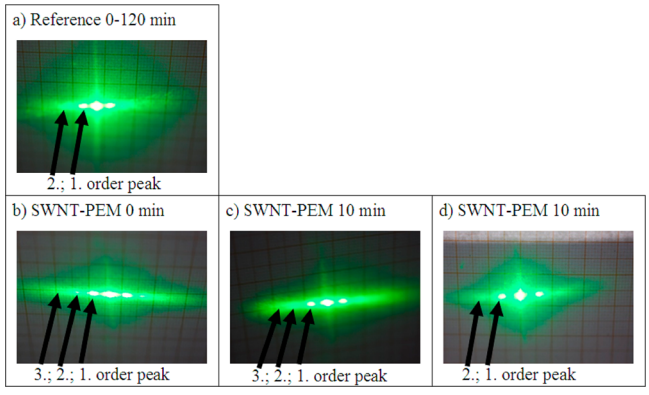

Figure 3. Change in optical diffraction patterns of released samples over time: (a) PEM reference, no change over time; (b) SWNT-containing PEM, immediately; third-order scattering peaks are present; (c) SWNT-containing PEM after 10 min; (d) SWNT-containing PEM after 2 h loss of the third-order scattering peak, and no change in intensity normal to the equatorial plane.

dx.doi.org/10.1021/jp3071458 | J. Phys. Chem. B 2012, 116, 12257–12262

explain this result, we expect that the compression force upon release changes the orientation of the SWNTs from a vertical to a parallel alignment. We explain the strong increase of the error bars upon the second release in Figure 2 with an increasing destruction of the film.

Kinetics in PEM with and without SWNTs. The time-dependent change of the PEM wrinkle wavelength (kinetics) was found to be much slower in the case of the PEM containing the SWNTs than that for the PEM without the SWNTs. For the PEM without the SWNTs, the kinetics was too fast to be measured with our setup. In the case of the PEM containing SWNTs, the scattering pattern changes its structure up to 2 h after the sample release. By a manual evaluation of the scattering pattern, one gets the impression that the wrinkling pattern on the surface becomes more disordered, since one scattering peak order gets lost, as shown in Figure 3.

Our results show that the initial wavelength of the reference PEM without the SWNTs (thickness similar to the PEM containing the SWNTs) is much more inhomogeneous (contains higher error bars) than the PEM containing the SWNTs. This effect is probably caused by a more homogeneous internal structure of the PEM containing hydrophobic SWNTs. On a hydrophobic substrate like PDMS, the hydrophobic SWNT−PDMS interaction leads to the buildup of a more homogeneous PEM.[30] Upon time passing by, the wrinkling wavelength of the PEM containing the SWNTs decreased in all samples, whereby the order of decrease was not very homogeneous, leading to high error bars; see Figure 4a. A possible reason for this might be the reorientation of the SWNTs, or other effects, such as film compression, filling of voids, fusion of cracks, or film thickening due to the constant force of the underlying deformed PDMS, which causes the film to creep slowly to its new equilibrium. Since the elastic modulus of matter depends on its composition and the orientation of molecules inside,[31] the elastic modulus of the PEM changes with time passing by, as shown in Figure 4b.

Kinetic Test with Pyrene-Labeled PSS. Since the PDMS maintains a constant force on a released or drawn PEM film to flatten out the wrinkles (in 10% elongated as well as released state),[9] we tried to monitor the effect of this mechanical force onto the inner structural change of the PE in a SWNT-free PEM film over 2 days (since pyrene is an electron emitter,[32] and SWNTs can act as an electron acceptor,[33] this test had to be done with the SWNT-free PEM). We monitored the pyrene fluorescence intensity ratio of the excimer (peak at 450 nm) to the peak 3 (peak at 400 nm) (also known as coiling index; see ref 30) over 2 days. Interestingly, the coiling index decreases in all samples over the applied time scale of 2 days, as can be seen in Figure 5. This decrease in coiling index can be interpreted as a

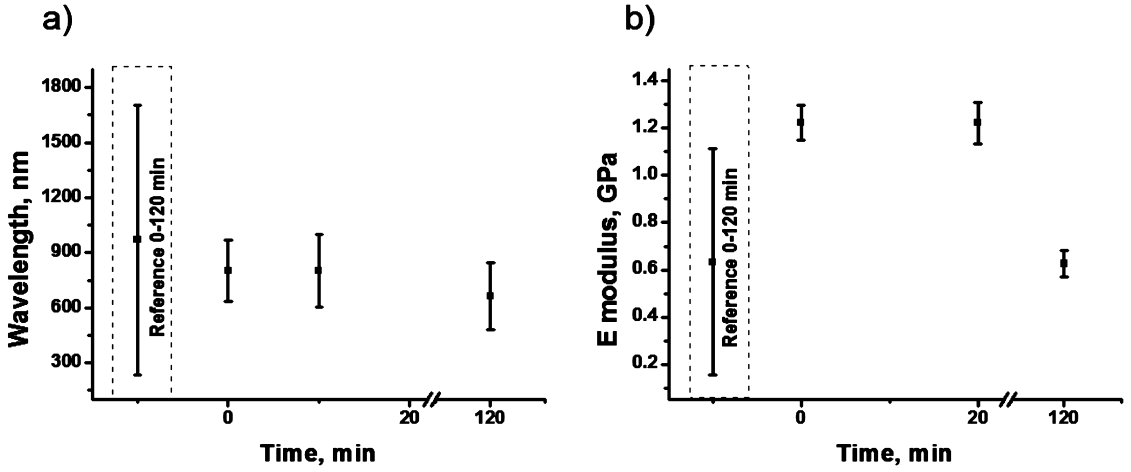

Figure 4. Time dependence of (a) wavelength and (b) *E* modulus in GPa of the SWNT−PEM samples. Reference sample shows no change over time, but high error bars. Due to the conversion from wavelength to *E* modulus, the error bars in (b) deviate from those in (a).

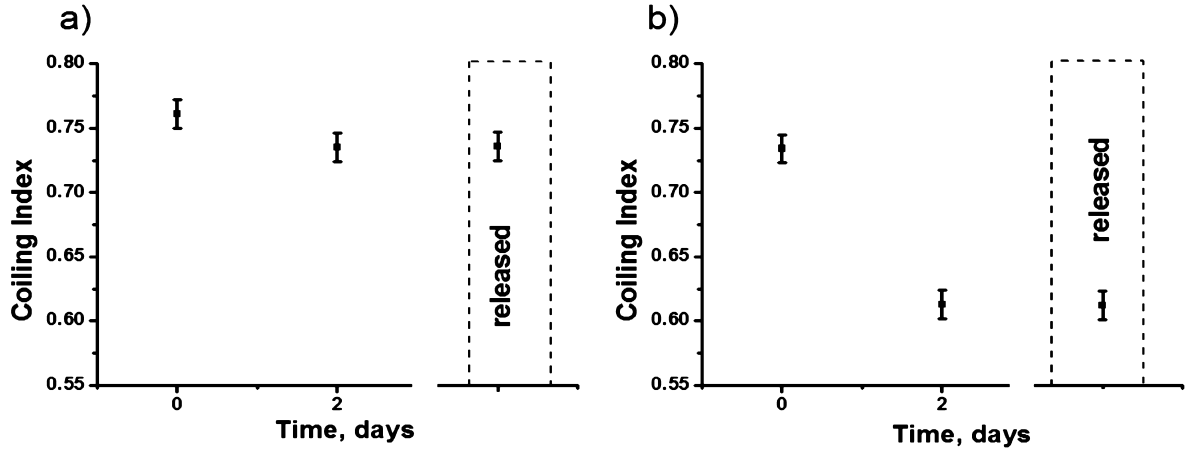

Figure 5. (a, b) Change in coiling index over time for two different samples, at 10% elongation and the released state. The decoiling is observed for both samples.

dx.doi.org/10.1021/jp3071458 | *J. Phys. Chem. B* 2012, 116, 12257−12262

decrease in the molecular coiling of the PE.[14] However, the degree of decrease was quite different; therefore, the error bars of the two investigated samples presented in Figure 5 simply show the error of the measurement method. This difference in degree of decrease originates probably from the fact that the PDMS slides were not plasma-etched and, therefore, quite hydrophobic. As a result, the hydrophilic polymers do not attach uniformly, and the degree of interaction between the PEM and the PDMS differs strongly from sample to sample.[15] We assume that the decoiling effect is also present in the case of the SWNT-containing PEM during structural shape adoption and also thereafter.

CONCLUSION

We showed that physically suspended SWNTs agglomerate upon incorporation into the PEM. We further showed that the SWNT orientation changes from anisotropic to isotropic upon uniaxial elongation of the PEM due to the influencing PDMS substrate. This behavior was recognized upon the first release. Upon a second release, the PEM was fairly destroyed, and the SWNT orientation was arbitrary.

Introducing SWNTs into the PEM prepared on hydrophobic PDMS results in the formation of a more homogeneous wrinkling structure. The macroscopic kinetics of the PEM wrinkles change also upon SWNT introduction. Instead of instant changes, the PEM responds over hours to the new structural equilibrium. We showed at last by the example of the pyrene-labeled PE that a long time kinetic effect based on the decoiling of PE within elongated and released PEM is also present in the case of non-SWNT-containing films. Here, this effect is very slow and leads to a decoiling of the PE molecules on the time scale of days.

ASSOCIATED CONTENT

Supporting Information

The Supporting Information contains (1) a drawing of the PSS-PY and the PDDA used, (2) a scheme of the experimental light-scattering setup, (3) spectra of the substrate, SWNT-free PEM, and SWNT-PEM upon elongation, (4) dichroic ratio and angular change of the SWNTs in elongated PEM, (5) scheme of linearly elongated PDMS as well as scattering pattern and microscopic images of 10% elongated SWNT-PEM, and (6) scheme of the suspected mechanism behind the counterintuitive effect of a decreasing SWNT order. This material is available free of charge via the Internet at http://pubs.acs.org.

AUTHOR INFORMATION

Corresponding Author

*E-mail: johannes.frueh@hit.edu.cn.

Author Contributions

The manuscript was written through contributions of all authors. All authors have given approval to the final version of the manuscript.

Notes

The authors declare no competing financial interest.

ACKNOWLEDGMENTS

We would like to thank Dr. Rumen Krastev for helpful discussions. We would also like to thank especially Jan von Szada Borowski for building the stretching device used in these tests. For financial support we would like to thank the Max-Plank Society, as well as Kyushu University, EU-FP7 Marie Curie Staff Exchange Scheme (No. 269159), and Harbin Institute of Technology. We also acknowledge financial support from DFG (Project KR3432/1-1).

REFERENCES

(1) Schönhoff, M. *Condens. Matter* **2003**, *15*, 1781−1808.
(2) Klitzing, R. v. *Phys. Chem. Chem. Phys.* **2006**, *8*, 5012−5033.
(3) Decher, G.; Hong, J. D.; Schmitt, J. *Thin Solid Films* **1992**, *210*−*211*, 831−835.
(4) Richter, R. P.; Berat, R.; Brisson, A. R. *Langmuir* **2006**, *22*, 3497−3505.
(5) Ross, E. E.; Spratt, T.; Liu, S.; Rozanski, L. J.; O'Brien, D. F.; Saavedra, S. S. *Langmuir* **2003**, *19*, 1766−1774.
(6) Brown, K. R.; Lyon, L. A.; Fox, A. P.; Reiss, B. D.; Natan, M. J. *Chem. Mater.* **2000**, *12*, 314−323.
(7) Nolte, A. J.; Rubner, M. F.; Cohen, R. E. *Macromolecules* **2005**, *38*, 5367−5370.
(8) Gao, C.; Leporatti, S.; Moya, S.; Donath, E.; Möhwald, H. *Langmuir* **2001**, *17*, 3491−3495.
(9) Nolte, A. J.; Treat, N. D.; Cohen, R. E.; Rubner, M. F. *Macromolecules* **2008**, *41*, 5793−5798.
(10) Hemmerle, J.; Roucoules, V.; Fleith, G.; Nardin, M.; Ball, V.; Lavalle, P.; Marie, P.; Voegel, J. C.; Schaaf, P. *Langmuir* **2005**, *21*, 10328−10331.
(11) Pavoor, P. V.; Bellare, A.; Strom, A.; Yang, D.; Cohen, R. E. *Macromolecules* **2004**, *37*, 4865−4871.
(12) Ladhari, N.; Hemmerle, J.; Haikel, Y.; Voegel, J.-C.; Schaaf, P.; Ball, V. *Appl. Surf. Sci.* **2008**, *255*, 1988−1995.
(13) Nakashima, T.; Zhu, J.; Qin, M.; Ho, S.; Kotov, N. *Nanoscale* **2010**, *2*, 2084.
(14) Frueh, J.; Koehler, R.; Moehwald, H.; Krastev, R. *Langmuir* **2010**, *26*, 15516−15522.
(15) Frueh, J. *Structural Change of Polyelectrolyte Multilayers under Mechanical Stress*; University of Potsdam: Potsdam, Germany, 2011; p 194.
(16) Tomonari, Y.; Murakami, H.; Nakashima, N. *Chem.—Eur. J.* **2006**, *12*, 4027−34.
(17) Mamedov, A. A.; Kotov, N. A.; Prato, M.; Guldi, D. M.; Wicksted, J. P.; Hirsch, A. *Nat. Mater.* **2002**, *1*, 190−194.
(18) Li, L.; Tedeschi, C.; Kurth, D. G.; Möhwald, H. *Chem. Mater.* **2004**, *16*, 570−573.
(19) Dietrich, S.; Haase, A. *Phys. Rep.* **1995**, *260*, 1−138.
(20) Decher, G. *Science* **1997**, *277*, 1232−1237.
(21) Schlenoff, J. B.; Dubas, S. T.; Farhat, T. *Langmuir* **2000**, 9968−9969.
(22) Frueh, J.; Reiter, G.; Möhwald, H.; He, Q.; Krastev, R. *Colloids Surf., A* **2012**, ASAP, COLSUA-D-12-00871R1.
(23) Fujigaya, T.; Haraguchi, S.; Fukumaru, T.; Nakashima, N. *Adv. Mater.* **2008**, *20*, 2151−2155.
(24) Murakami, Y.; Einarsson, E.; Edamura, T.; Maruyama, S. *Carbon* **2005**, *43*, 2664−2676.
(25) Fraser, R. D. B. *J. Chem. Phys.* **1953**, *21*, 1511−1515.
(26) Kawamoto, H. *Proc. IEEE* **2006**, *90*, 460−500.
(27) Stafford, C. M.; Harrison, C.; Beers, K. L.; Alamgir, K.; Amis, E. J.; VanLandingham, M. R.; Kim, H.-C.; Volksen, W.; Miller, R. D.; Simony, E. E. *Nat. Mater.* **2004**, *3*, 545−550.
(28) Lu, C.; Doench, I.; Nolte, M.; Fery, A. *Chem. Mater.* **2006**, *18*, 6204−6210.
(29) Köhler, R.; Dönch, I.; Ott, P.; Laschewsky, A.; Fery, A.; Krastev, R. *Langmuir* **2009**, *25*, 11576−11585.
(30) Park, J.; Hammond, P. T. *Macromolecules* **2005**, *38*, 10542−10550.
(31) Takayanagi, M.; Imada, K.; Kajiyama, T. *J. Polym. Sci., Part C* **1967**, *15*, 263−281.
(32) Chudek, J. A.; Foster, R.; Page, F. *J. Chem. Soc., Faraday Trans. 1* **1987**, *83*, 2641−2645.
(33) Kymakis, E.; Amaratunga, G. A. J. *Rev. Adv. Mater. Sci.* **2005**, *10*, 300−305.